Precise determination of the bond percolation thresholds and finite-size scaling corrections for the sc, fcc, and bcc lattices

Christian D. Lorenz and Robert M. Ziff
Department of Chemical Engineering, University of Michigan, Ann Arbor, Michigan 48109-2136
(Received 22 August 1997)

Extensive Monte Carlo simulations were performed to study bond percolation on the simple cubic (sc), face-centered-cubic (fcc), and body-centered-cubic (bcc) lattices, using an epidemic approach. These simulations provide very precise values of the critical thresholds for each of the lattices: $p_c(\mathrm{sc}) = 0.248\,812\,6 \pm 0.000\,000\,5$, $p_c(\mathrm{fcc}) = 0.120\,163\,5 \pm 0.000\,001\,0$, and $p_c(\mathrm{bcc}) = 0.180\,287\,5 \pm 0.000\,001\,0$. For p close to p_c, the results follow the expected finite-size and scaling behavior, with values for the Fisher exponent τ (2.189 ± 0.002), the finite-size correction exponent Ω (0.64 ± 0.02), and the scaling function exponent σ (0.445 ± 0.01) confirmed to be universal. [S1063-651X(98)04601-7]

PACS number(s): 64.60.Ak, 64.60.Cn, 64.70.Pf

I. INTRODUCTION

Percolation theory is used to describe a variety of natural physical processes, which have been discussed in detail by Stauffer and Aharony [1] and Sahimi [2]. In two-dimensional percolation, either exact values or precise estimates are known for the critical thresholds and other related coefficients and exponents [3–6].

However, three-dimensional lattices are relevant for most natural processes. The most common of these are the simple cubic (sc), the face-centered-cubic (fcc), and the body-centered-cubic (bcc) lattices. The percolation thresholds for these lattices are not known exactly and the estimates that have been determined for the latter two lattices are much less precise than the values that have been found for typical two-dimensional systems.

An exception is the case of the sc lattice, where fairly precise values have been determined. A number of years ago, Ziff and Stell carried out a study of three-dimensional percolation for the site and bond percolation on the sc lattice [7]. The values $p_c = 0.248\,812 \pm 0.000\,002$ and $p_c = 0.311\,605 \pm 0.000\,010$ were found for bond and site percolation, respectively. The behavior for p away from p_c was also studied and it was found that the critical exponents can be described by the consistent set $\tau = 116/53 \approx 2.1887$, $\sigma = 24/53 \approx 0.4528$, and $\nu = 7/8$, with errors ± 0.001, ± 0.001, and ± 0.008, respectively. However, this work, which used a growth method essentially equivalent to the epidemic approach, remained unpublished as an internal report only [7].

In a more recent work, Grassberger found $p_c = 0.248\,814 \pm 0.000\,003$ and $p_c = 0.311\,604 \pm 0.000\,006$ for bond and site percolation (respectively) on the sc lattice [8], using an epidemic analysis [9]. The precise agreement between these two independent works provides strong evidence that the procedures, random-number generators, error analyses, etc., implemented by both groups of authors are correct. Previous to these two works, p_c was known only to about four significant figures, as discussed below. It is important to know p_c very precisely so that other critical properties can be studied without bias.

For bond percolation on the fcc and bcc lattices, the most accurate values appear to be $p_c = 0.1200 \pm 0.0002$ and $p_c = 0.1802 \pm 0.0002$, respectively, recently found by van der Marck [10] using the average crossing probability method [1]. Additional literature values are listed below. These thresholds are not precise enough for a study we have been carrying out on the universal excess cluster numbers in three-dimensional systems [11] and as a consequence we have conducted the present work.

Here we use a growth or epidemic analysis to obtain high-precision values for the percolation thresholds of the sc, fcc, and bcc lattices. We reaffirm that three-dimensional percolation follows the hypothesized finite-size and scaling behavior, and estimate the exponents and coefficients that enter into the finite-size and scaling functions.

In the following sections, we discuss the simulation that we used to grow the percolation clusters and obtain our data. Then we present and briefly discuss the results that we obtained from our simulations.

II. SIMULATION METHOD

We used a Monte Carlo simulation of bond percolation on each of the three-dimensional lattices. This simulation employed the so-called Leath growth algorithm [12] to generate individual percolation clusters. The cluster was started at a seeded site that was centrally located on the lattice. From this site, a cluster was grown to neighboring sites by occupying the connecting bonds with a certain probability p or leaving them unoccupied with a probability $1-p$. The unit vectors that were used to locate the neighboring sites for each lattice are summarized in Table I. All of these clusters were allowed to grow until they reached an upper cutoff, at which point any cluster that was still growing was halted. This cutoff was 2^{21} (2 097 152) wetted sites for the sc lattice and 2^{20} (1 048 576) wetted sites for the fcc and bcc lattices. The size of the cluster was characterized by the number of wetted sites rather than the occupied bonds of the clusters since the former figures directly in the growth algorithm procedure.

In order to grow such large clusters, our simulation used the data-blocking scheme [13], in which large lattice is divided into smaller blocks and memory is assigned to a block only after the cluster has grown into it. In this case, the

TABLE I. Unit vectors used to describe the neighbors in the sc, fcc, and bcc lattices.

Lattice	Vectors
sc	(1,0,0), (0,1,0), (0,0,1), (−1,0,0), (0,−1,0), (0,0,−1)
fcc	(1,1,0), (1,−1,0), (−1,−1,0), (−1,1,0), (1,0,1), (−1,0,1), (1,0,−1), (−1,0,−1), (0,1,1), (0,−1,1), (0,1,−1), (0,−1,−1)
bcc	(1,1,1), (1,1,−1), (−1,1,1), (−1,1,−1), (−1,−1,1), (−1,−1,−1), (1,−1,1), (1,−1,−1)

lattice, which has dimensions of $2048\times2048\times2048$, was divided into 64^3 blocks of dimensions of size $32\times32\times32$. Bit mapping was also used to reduce the memory load of the large lattices. The upper six bits of each coordinate were used to tell where in the memory that block is mapped. The lower five bits of the y and z coordinates tell the memory which word and the lower five bits of the x coordinate tell the memory which bit of that word is used to store the site. With such a large lattice and the cutoffs we used, none of the clusters saw the lattice boundary, so there were no boundary effects.

The simulation counted the number of clusters that closed in a range of $(2^n,2^{n+1}-1)$ sites for $n=0,1,\ldots$ and recorded this number in the nth bin. If a cluster was still growing when it reached the upper cutoff, it was counted in the last (20th or 21st) bin. The simulation also kept track of the average number of occupied bonds and the average number of unoccupied bonds for clusters in each bin range, for reasons discussed below.

Random numbers were generated by the four-tap shift-register rule $x_n=x_{n-471}\oplus x_{n-1586}\oplus x_{n-6988}\oplus x_{n-9689}$, where $\oplus$ is the exclusive-or operation, which we have used (with apparent success) in numerous previous studies (e.g., [4,5]).

III. RESULTS

A. Fisher exponent τ

Using the data obtained from the simulation, the number of clusters grown to a size greater than or equal to size s can be deduced. The probability of growing clusters with the number of wetted sites greater than or equal to s, $P(s,p)$, when operating at the critical threshold ($p=p_c$) and neglecting finite-size effects is predicted to follow [1]

$$P(s,p_c)\sim As^{2-\tau}. \tag{1}$$

In Fig. 1 data from our simulation plotted on a log-log plot show good agreement with this equation. However, for small clusters, there is a clear nonlinear region, which represents the finite-size effect. For large s, the curves also become nonlinear, resulting from growing the clusters at values of p away from p_c. Values of p that are greater than p_c produce curves that increase for large s and values of p below p_c cause curves to decrease.

Such behavior is similar to that seen in an epidemic analysis of a transition of interacting particle systems and indeed the cluster growth procedure is in fact essentially such a process. The only difference is that, in the usual epidemic analysis [9], one plots the growth probability as a function of time (generation or chemical distance number for percolation), while here we plot that probability as a function of size. However, since the size scales with time, the two approaches are equivalent.

The slope of the linear portion of the curves shown in Fig. 1 is equal to $2-\tau$, where τ is the Fisher exponent [14]. However, due to the nonlinear portions of the curves and the uncertainty of which p is precisely at the critical threshold, it is difficult to accurately deduce τ from these plots. To make the behavior more pronounced, we plot difference between the data and a straight line of slope $2-\tau$ in Fig. 2, for the fcc lattice and different values of p. Here the correct value of τ produces a horizontal central portion of the curve. Applying this analysis for all three lattices yields $\tau=2.189\pm0.002$. Figure 3 shows the effect of using slightly larger or smaller values of τ for the fcc lattice.

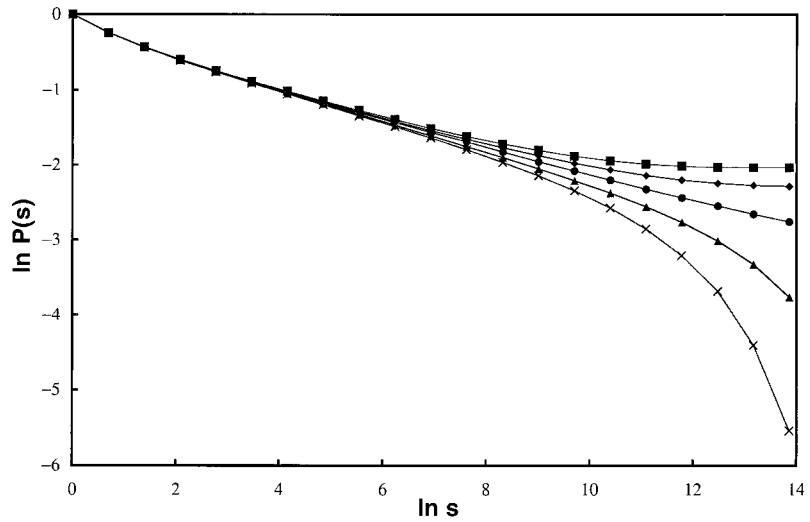

FIG. 1. Plot of the raw simulation results on a log-log plot. These data are from the fcc lattice and each of the five curves represent a different value of p: 0.1206 (square), 0.1204 (diamond), 0.1202 (circle), 0.1200 (triangle), and 0.1198 (cross). Nonlinearities are caused by finite-size effects (small s) and p not equaling p_c (large s).

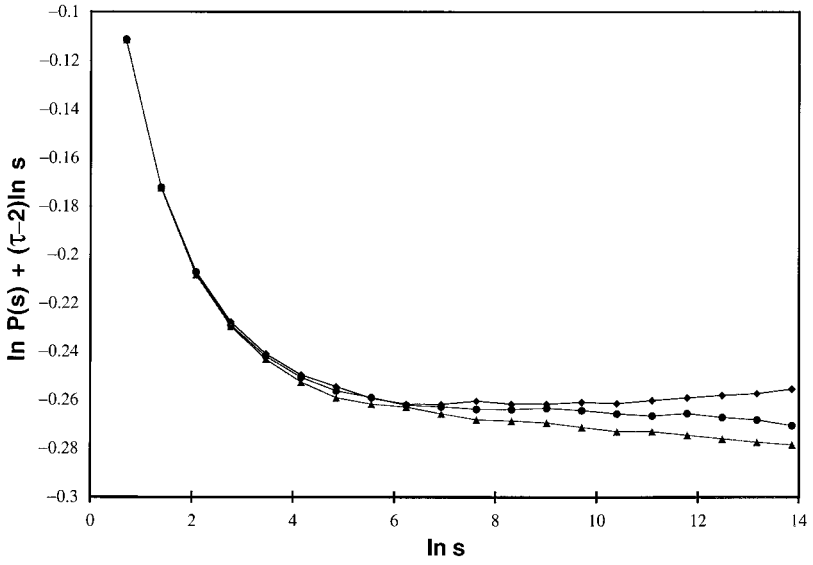

FIG. 2. Determination of the Fisher exponent τ by plotting $\ln s^{\tau-2}P(s,p_c)$ vs $\ln s$. These curves show data from the simulations of a fcc lattice and each curve represents a different value of p: 0.120 165 (diamond), 0.120 162 (circle), and 0.120160 (triangle). These curves were produced using a value of $\tau=2.189$, which produced the best horizontal curve for all three lattices.

B. Finite-size corrections

In order to account for the small clusters, the finite-size correction must be added to Eq. (1). Then P is predicted to follow

$$P(s,p_c)\sim As^{2-\tau}(A+Bs^{-\Omega}+\cdots), \tag{2}$$

where Ω is the first correction-to-scaling exponent [15]. Like Eq. (1), Eq. (2) is only valid at the critical threshold. At the correct value of Ω, Eq. (2) predicts there will be a linear relationship between $s^{\tau-2}P(s,p_c)$ and $s^{-\Omega}$. Figure 4 shows plots between these two quantites for the sc, fcc, and bcc lattices, respectively. The values of Ω that produced the best linear fit are summarized in Table II. The slope of the curves gives the value for the coefficient B in Eq. (2) and the intercept gives A in Eqs. (1) and (2). The values we found are summarized in Table III. Note that the last data point is shown on each of these plots, but they have been left out of linear fits because they represent clusters of only two sites, too small to be described by just the first term of the finite-size corrections series.

C. Percolation thresholds

In Fig. 1 we show the effect that values of p away from p_c have on the data for large clusters. In order to account for the behavior when $p\neq p_c$, a scaling function needs to be included in P. The behavior is then represented by

$$P(s,p_c)\sim As^{2-\tau}f((p-p_c)s^{\sigma}), \tag{3}$$

which is valid rigorously in the scaling limit as $s\to\infty$, $p\to p_c$, such that $(p-p_c)s^{\sigma}=\text{const}$ [1]. Because p is close to p_c, we can expand $f(x)$ in a Taylor series

$$f((p-p_c)s^{\sigma})\sim 1+C(p-p_c)s^{\sigma}+\cdots . \tag{4}$$

Equation (3) and (4) describe how $s^{\tau-2}P(s,p)$ deviates from a constant value for large s when p is close to p_c. Figures 5(a), 5(b), and 5(c) show the plots of $s^{\tau-2}P(s,p)$ vs s^{σ} for the sc, fcc, and bcc lattices, respectively. For these plots, we used the value of $\sigma=0.453$ from [7] and the linearity of the plots confirms that it is a good value. These plots show a steep decline, which is the finite-size effect, followed by a

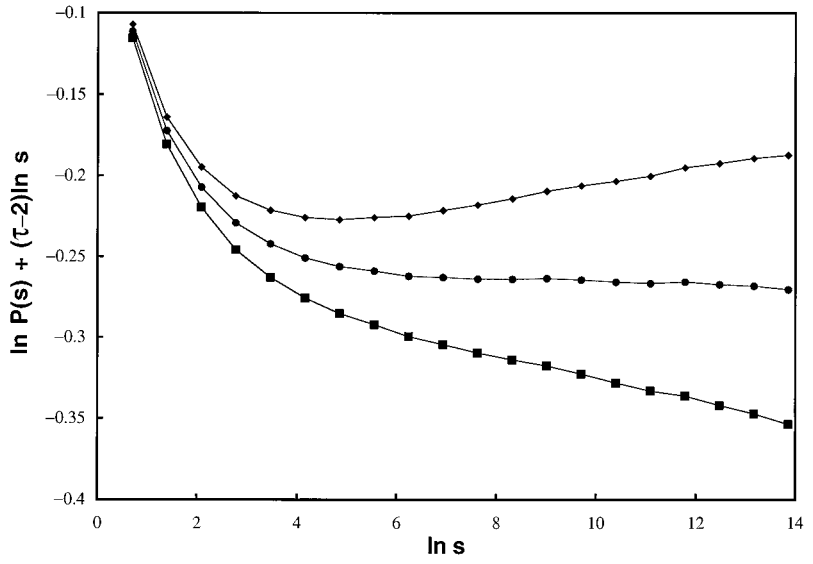

FIG. 3. Effect of varying τ on the central curve of Fig. 2 (fcc lattice). These curves (all at $p=0.120\,162$, which is close to p_c) compare three different values of τ: 2.192 (diamond), 2.189 (circle), and 2.186 (square). The best horizontal fit is clearly produced by using the middle value.

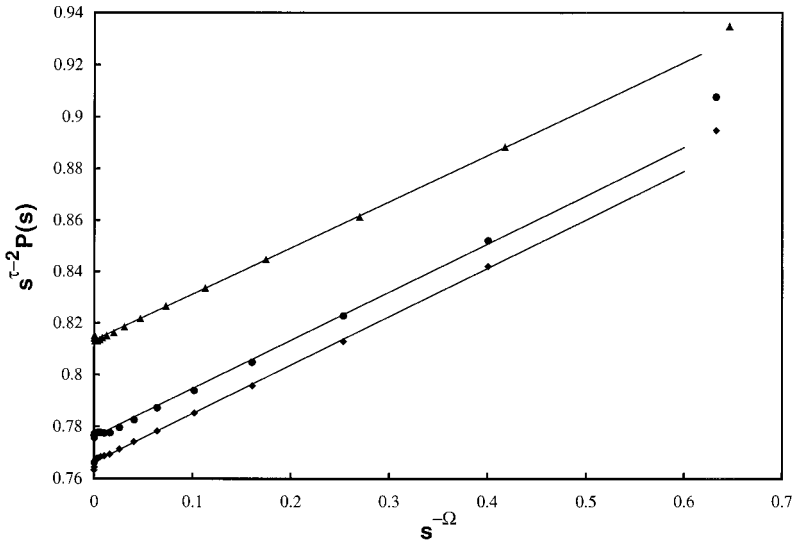

FIG. 4. Plot to determine the finite-size correction predicted by Eq. (2), for the sc (triangle), bcc (circle), and fcc (diamond) lattices. The values of Ω, A, and B are summarized in Tables II and III. The last points of each curve, which represented clusters of just two wetted sites, were left out of the curve fit. Deviations from linearity for large s are caused by p being slightly different from p_c.

mostly linear region as predicted by Eq. (4). The linear portions of the curve become more nearly horizontal as the chosen value of p gets closer to p_c. The value for the critical threshold can be deduced by interpolating from these plots. For the three lattices considered here, we thus find

$$p_c(\text{sc}) = 0.248\ 812\ 6 \pm 0.000\ 000\ 5, \tag{5a}$$

$$p_c(\text{fcc}) = 0.120\ 1635 \pm 0.000\ 001\ 0, \tag{5b}$$

$$p_c(\text{bcc}) = 0.180\ 287\ 5 \pm 0.000\ 001\ 0; \tag{5c}$$

A more formal method of carrying out this interpolation can be obtained by plotting the slopes of the curves, shown in Figs. 5(a)–5(c), vs p. From Eqs. (3) and (4), it follows that

$$\frac{\partial(s^{\tau-2}P(s,p))}{\partial(s^{\sigma})} = C(p-p_c)+\cdots, \tag{6}$$

which implies that the value of the critical threshold can be calculated from the x intercept of this plot, as shown in Fig. 6. Figures 5(a) and 6 yield consistent values of the critical threshold for the sc lattice.

D. Scaling function

The linearized scaling function, as shown in Eqs. (3) and (4), can be studied efficiently by the following procedure. From Eqs. (3) and (4) it follows that

$$\frac{\partial P(s,p)}{\partial p} = ACs^{2-\tau+\sigma}+\cdots. \tag{7}$$

Equation (7) shows that we could determine $2-\tau+\sigma$ and AC directly from a measurement of the derivative $\partial P/\partial p$ as a function of s.

To develop a formula for this derivative, we consider the formal expression for the probability of growing a cluster containing n occupied bonds and t vacant (perimeter) bonds:

$$P_{n,t} = g_{n,t}p^n(1-p)^t, \tag{8}$$

where $g_{n,t}$ is the number of distinct clusters configurations with n occupied and t vacant bonds. From Eq. (8) we can write the probability of growing a cluster of size greater than or equal to s as

$$P(s,p) = \sum_n \sum_t g_{n,t}p^n(1-p)^t, \tag{9}$$

where the sum is over all n and t such that the number of wetted sites is greater than or equal to s.

Differentiating Eq. (9) with respect to p gives

$$\frac{\partial P(s,p)}{\partial p} = \sum_n \sum_t g_{n,t}p^n(1-p)^t\left(\frac{n}{p}-\frac{t}{1-p}\right), \tag{10}$$

which can be simplified to the final form

$$\frac{\partial P(s,p)}{\partial p} = \frac{\langle n\rangle}{p}-\frac{\langle t\rangle}{1-p}, \tag{11}$$

where $\langle n\rangle$ and $\langle t\rangle$ are the average number of occupied and unoccupied bonds, respectively, over all clusters of size greater than or equal to s. For a Monte Carlo estimate of this

TABLE II. Values of the universal finite-size correction exponent Ω and the scaling function exponent σ for the sc, fcc, and bcc lattices. (σ was not found for the sc lattice.)

Lattice	Ω	σ
sc	0.63	
fcc	0.66	0.4453
bcc	0.66	0.4433

TABLE III. Nonuniversal coefficients for finite-size correction and the scaling function of the sc, fcc, and bcc lattices. (C was not found for the sc lattice.)

Lattice	A	B	C
sc	0.813	0.178	
fcc	0.767	0.186	7.95
bcc	0.776	0.187	5.57

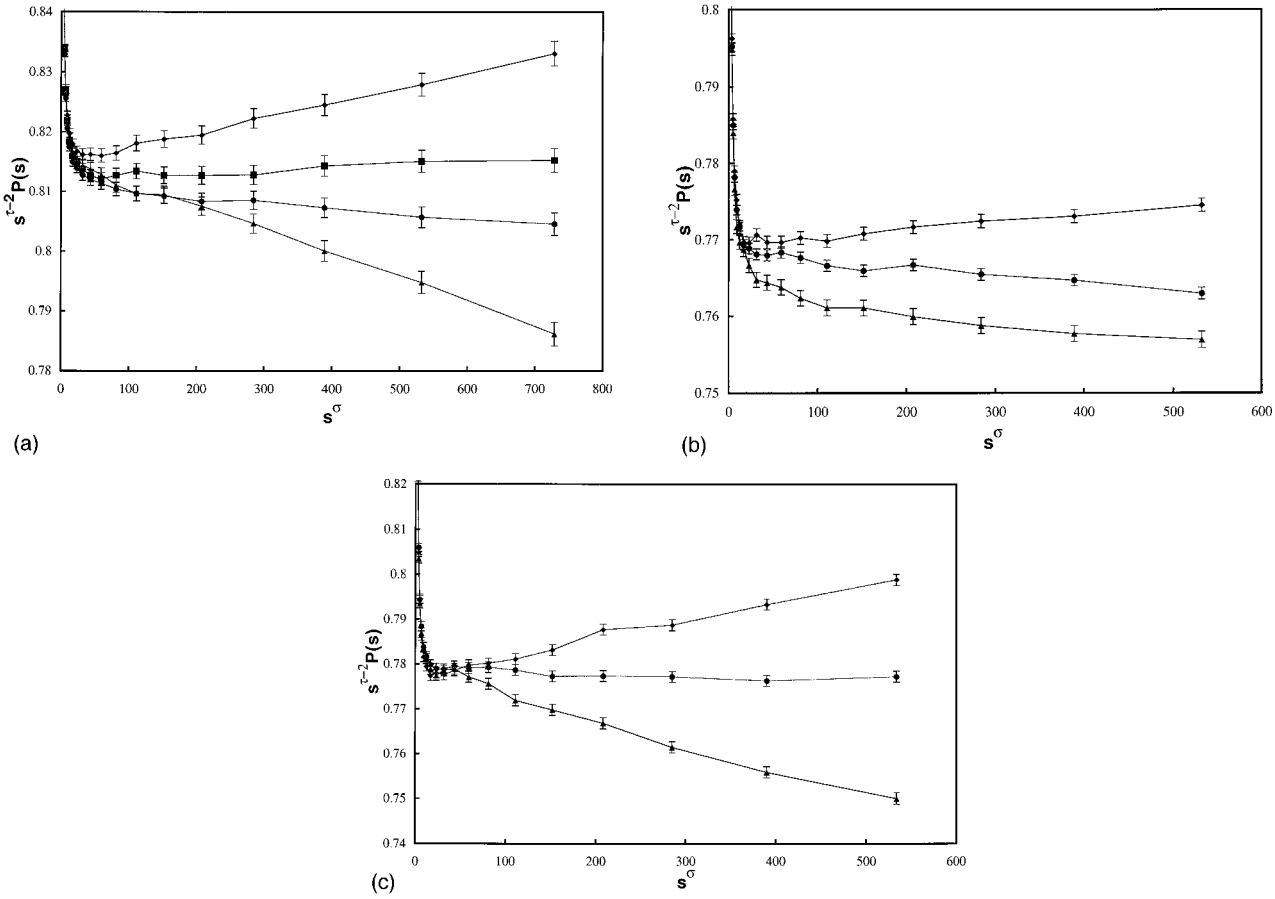

FIG. 5. Plot of $s^{\tau-2}p(s)$ vs s^{σ}. The linearity for large s demonstrates the validity of Eqs. (3) and (4). The value of p that produces the best horizontal fit yields the critical threshold. (a) shows the data from the sc lattice and each curve shows a different value of p: 0.248 820, 0.248 814, 0.248 810, and 0.248 800. (b) shows the data from the fcc lattice and the values of p shown are 0.120 165, 0.120 162, and 0.120 160. (c) shows the data from the bcc lattices and the values of p are 0.180 300, 0.180 287 5, and 0.180 275 0 (top to bottom in all cases).

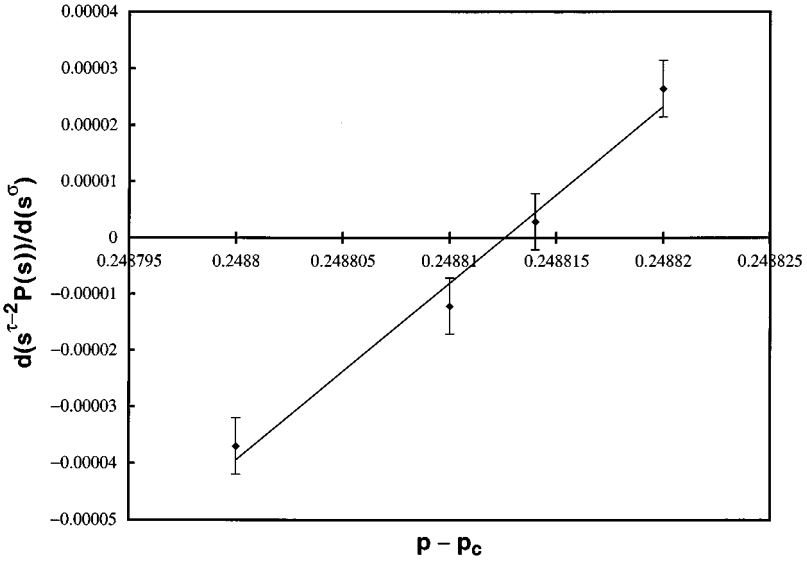

FIG. 6. Plot of the slope of the linear portions of the curves shown in Fig. 5(a) as a function of p. The x intercept gives the value of the critical threshold for the sc lattice.

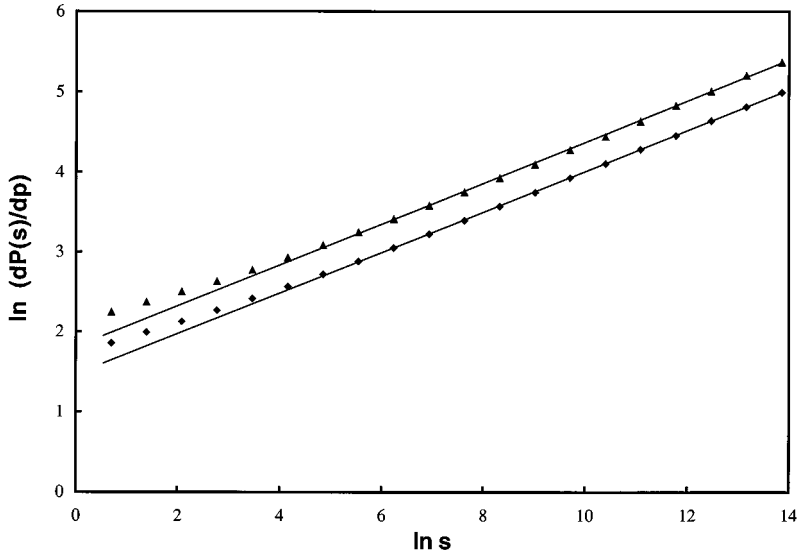

FIG. 7. Determination of σ and C using $\partial P/\partial p$ calculated from Eq. (11). By fitting the last 15 data points to Eq. (7), $2-\tau+\sigma$ can be found from the slope of these curves and AC can be found from the y intercept. The resulting values of σ and C (using τ and A determined above) for the fcc (triangle) and bcc (diamond) lattices are summarized in Tables II and III, respectively.

derivative, we simply use $\langle n \rangle$ and $\langle t \rangle$ averaged over the sample of clusters. The values for these averages were recorded by our simulations and were then used with Eq. (11) to calculate the derivative.

Figure 7 shows a plot of the measured derivative (11) vs s for the fcc and bcc lattices. From the slopes and intercepts, and using the values of A and τ determined above, we can deduce σ and C. For σ we find 0.445 ± 0.01 for both cases, which is consistent with [7], and the values of C we find are given in Table III.

Another application of the derivative (11) is that it can be used to produce new curves at values of p near p_c that resemble the curves seen in Figs. 5(a)–5(c), by virtue of a Taylor expansion

$$P(s,p_2)=P(s,p_1)+(p_2-p_1)\left.\frac{\partial P(s,p)}{\partial p}\right|_{p=p_1}, \qquad (12)$$

where the last derivative is determined using Eq. (11). This ''shifting'' of the data is useful for correcting results taken close to, but not precisely at, p_c, without carrying out a new set of time-consuming simulations.

IV. DISCUSSION OF RESULTS

A. Fisher exponent τ

Our results show excellent agreement with the expected relationship for the number of cluster of size greater than or equal to s, which is shown in Eq. (1). The only nonlinear portions of the curve on a log-log plot occur when s is either small or large, which is where Eq. (1) is not valid. These nonlinearities are caused by the finite-size effect (small s) and the departure of p from p_c (large s).

The value of τ was found by comparing curves that were similar to those shown in Figs. 2 and 3, finding the value that produced the most nearly horizontal curve. As can be seen in Figs. 2 and 3 for the fcc lattice, the reported value of $\tau = 2.189$ [7] gives the best horizontal curve. This value of τ also provides the best horizontal curves for the other two lattices, showing universality (with error bars of ± 0.002). This value of τ is also consistent with the values given by Stauffer and Aharony (2.18) [1] and Nakanishi and Stanley (2.19) [16].

B. Finite-size corrections

In Fig. 4 our data show excellent agreement with the prediction described by Eq. (2). It is expected that the exponent Ω is a universal quantity, while the coefficients A and B are different for the three different lattices. These expectations were borne out by our results showing the best fit of data for all three lattices occurred at approximately the same value of Ω (0.64 ± 0.02), as shown in Table II, but different values of the coefficients as given in Table III. Our value for Ω is significantly larger than the value reported by Nakanishi and Stanley ($\Omega = 0.40$) [16]. We believe this discrepancy is due to their using less precise values of the critical exponents, which leads to more inherent error in Ω, and carrying out significantly fewer simulations, as were feasible at the time that that work was done.

C. Percolation thresholds

In Figs. 5(a)–5(c), our data show excellent agreement with the predicted relationship as described by Eqs. (3) and (4). The curves show the finite-size effects for small s and then become linear. The linear portion of the curves become more nearly horizontal as the value of p approaches p_c, which is also predicted by the equations.

Our values for the critical thresholds (5) are consistent with most previous works. The critical threshold for the fcc lattice has been reported as 0.1200 ± 0.0002 [10] and 0.119 [1]. The critical threshold for the bcc lattice has been reported as 0.1802 ± 0.0002 [10] and 0.1803 [1]. The critical threshold for the sc lattice has been reported as $0.248\,812 \pm 0.000\,002$ [7], $0.248\,814 \pm 0.000\,003$ [8], 0.2488 [1], 0.24875 ± 0.00013 [17], 0.2488 ± 0.0002 [18], and 0.2487 ± 0.0002 [10]. A number of years ago the higher values 0.2492 ± 0.0002 [19] and 0.2494 ± 0.0001 [20] were reported, but these have since been recognized as probably erroneous due to a flaw in programming [21].

D. Scaling function

One expects that the value of the scaling function exponent σ should be a universal quantity while the coefficient C should be different for each of the lattices. Values of these quantities were only calculated for the fcc and bcc lattices because in the sc lattice simulations we did not record the values of $\langle n \rangle$ and $\langle t \rangle$. The same value of σ (0.445 ± 0.01) produced the best fit for both lattices. This value is significantly smaller than the value reported by Nakanishi and Stanley (0.504 ± 0.030) [16], but it is consistent with the values given by Ziff and Stell [7] (0.453 ± 0.001) and Stauffer and Aharony [1] (0.45). The values for the coefficient C, which are summarized in Table III, were different for the two lattices. Thus these results confirm the expectations.

V. CONCLUSION

Our work has produced the bond percolation critical threshold values given in Eq. (5). For the fcc and bcc lattices these results are at least two orders of magnitude more precise than previous values, while for the sc lattice the result is four times more precise. We find critical exponents consistent with those given in [7], and a more precise value of the correction-to-scaling exponent Ω than previously known. This increased precision is the result of having conducted extensive simulations with an inherently efficient procedure (the epidemic method [9]) along with programming techniques that allow one to simulate very large lattices [13]. The results of this work allow other properties of three-dimensional percolation on these lattices to be studied equally precisely.

Because all of this work was performed in a relatively short amount of time, we believe that the epidemic approach is a more efficient way to find the critical threshold than the conventional crossing-probability methods. However, we did not make a direct time comparison of two methods. Note that the epidemic growth algorithm used here can also be used to study systems of any dimension, unlike hull methods [4,22,23], which are limited to two dimensions.

Our measurements of $P(s,p)$ for all s (except the smallest values) and for p very close to p_c can be summarized in a single equation

$$P(s,p) = s^{\tau-2}(A + Bs^{-\Omega})[1 + C(p - p_c)s^{\sigma}], \qquad (13)$$

with all constants and exponents determined by our simulations. Although this equation mixes finite-size and bulk scaling forms, it provides a very accurate fit of the data in the regime we studied.

ACKNOWLEDGMENTS

This material is based upon work supported by the U.S. National Science Foundation under Grant No. DMR-9520700.

[1] D. Stauffer and A. Aharony, *An Introduction to Percolation Theory*, revised 2nd ed. (Taylor and Francis, London, 1994).
[2] M. Sahimi, *Applications of Percolation Theory* (Taylor and Francis, London, 1994).
[3] M. F. Sykes and J. W. Essam, J. Math. Phys. **5**, 1117 (1964).
[4] R. M. Ziff and P. N. Suding, J. Phys. A **30**, 5351 (1997).
[5] R. M. Ziff, Phys. Rev. Lett. **69**, 2670 (1992).
[6] B. Nienhuis, J. Phys. A **15**, 199 (1982).
[7] R. M. Ziff and G. Stell, University of Michigan Report No. 88-4, 1988 (unpublished).
[8] P. Grassberger, J. Phys. A **25**, 5867 (1992).
[9] P. Grassberger and A. de la Torre, Ann. Phys. (N.Y.) **122**, 373 (1979).
[10] S. C. van der Marck, Phys. Rev. E **55**, 1514 (1997).
[11] C. D. Lorenz and R. M. Ziff (unpublished).
[12] P. L. Leath, Phys. Rev. B **14**, 5046 (1976).
[13] R. M. Ziff, P. T. Cummings, and G. Stell, J. Phys. A **17**, 3009 (1984).
[14] M. E. Fisher, Physics (Long Island City, NY) **3**, 255 (1967).
[15] J. Hoshen, D. Stauffer, G. H. Bishop, R. J. Harrison, and G. P. Quinn, J. Phys. A **12**, 1285 (1979).
[16] H. Nakanishi and H. E. Stanley, Phys. Rev. B **22**, 2466 (1980).
[17] P. Grassberger, J. Phys. A **19**, L241 (1986).
[18] J. Adler, Y. Meir, A. Aharony, and A. B. Harris, Phys. Rev. B **41**, 9183 (1990).
[19] S. Wilke, Phys. Lett. **96A**, 344 (1983).
[20] D. Stauffer and J. G. Zabolitzky, J. Phys. A **19**, 3705 (1986).
[21] D. Stauffer, J. Adler, and A. Aharony, J. Phys. A **27**, L475 (1994).
[22] M. Rosso, J.-F. Gouyet, and B. Sapoval, Phys. Rev. B **32**, 6053 (1986).
[23] R. M. Ziff and B. Sapoval, J. Phys. A **18**, L1169 (1986).